Photooxidation of CH_3Cl on $TiO_2(110)$: A Mechanism Not Involving H_2O

G. Lu, A. Linsebigler, and J. T. Yates, Jr.*

Surface Science Center, Department of Chemistry, University of Pittsburgh, Pittsburgh, Pennsylvania 15260

Received: July 6, 1994; In Final Form: September 2, 1994[⊗]

A model reaction has been employed to investigate the mechanism for the photooxidation of chlorinated hydrocarbons on TiO_2 semiconductor surfaces. Utilizing modern surface science techniques, the roles of surface defects (surface oxygen vacancies), adsorbed molecular oxygen, and surface hydroxyl groups have been studied on $TiO_2(110)$ in connection with the photooxidation of methyl chloride. The coverage of each of the above species can be characterized and well controlled. The presence of surface defects and molecular oxygen adsorbed on the defect sites is essential for the photoreaction to initiate and to proceed. Surface hydroxyl groups do not oxidize methyl chloride under UV irradiation. However, adsorbed water molecules do participate in the photoreaction in the presence of adsorbed molecular oxygen. The photooxidation has an energy threshold of 3.1 eV, showing that the reaction is induced by TiO_2 band-gap excitation. These results show that under our experimental conditions the substrate-mediated excitation of molecular oxygen plays the more important role in the photooxidation of methyl chloride on TiO_2 surfaces.

Introduction

The photooxidation of organic compounds on TiO_2 surfaces has been extensively investigated.[1,2] The significance of such studies lies in the potential application of TiO_2 as a photocatalyst for the total mineralization of environmentally harmful organic compounds.[2-4] The process is initiated by the band-gap excitation of the TiO_2 particles under UV irradiation. The electrons and holes thus produced diffuse to the surface and react with surface species. In aqueous suspension systems, it is believed that electrons are trapped at surface defect sites (Ti^{3+}) and can be removed by reactions with adsorbed molecular O_2 to produce O_2^-, or with H^+ to produce H_2, etc. Surface hydroxyl groups react with the holes and produce $^{\bullet}OH$ radicals. The photogenerated $^{\bullet}OH$ radical derived from water has been postulated to be the oxidizing agent which controls the kinetics of the overall oxidation process.[5,6] This mechanism is based on the identification of hydroxylated reaction intermediates,[7-13] the EPR detection of $^{\bullet}OH$ radical species,[14-16] and the kinetic effect of surface hydroxylation on the photooxidation.[10,17,18]

However, several recent studies have questioned whether this mechanism may be universally applied to all TiO_2-based photocatalytic oxidation systems (liquid or gas phase).[19-23] Especially, the assertion that the hydroxyl radicals are solely responsible for the photooxidation process has been challenged. In a diffuse reflectance flash photolysis experiment, Draper and Fox could not detect any of the expected $^{\bullet}OH$ adduct intermediates and suggested direct interactions between the holes and the adsorbates.[19] Okamoto et al.[20] and Anpo et al.[21] suggested the involvement of O_2-derived radical species ($^{\bullet}O_2^-$, $HO_2^{\bullet}$, H_2O_2, etc., formed by capturing the photogenerated electrons) during the photooxidation of organic compounds. Recent studies on the photooxidation of 4-chlorophenol[22] and trichloroethylene[23] have reported total photooxidation even in the absence of water and surface hydroxyl groups. These studies suggested that the photooxidation process on TiO_2 is not exclusively achieved through $^{\bullet}OH$ radicals that are generated by reactions between surface hydroxyl groups and the photogenerated holes. The role of O_2 is believed to be more than merely an electron scavenger.[22] However, the extent of O_2 participation in the photooxidation process has not been defined. The present investigation addresses these important issues using a well-defined $TiO_2(110)$ single crystal surface and modern surface science measurement methods. Questions about the role of surfaces compared to the role of reactions in solution do not exist in this work done in ultrahigh vacuum.

Methyl chloride is chosen as a model chlorinated hydrocarbon molecule for simplicity. The (110) surface is the most stable face of the rutile TiO_2 single crystal. On the well-characterized $TiO_2(110)$ surface we are able to accurately measure and control the coverage of surface defects, adsorbed molecular oxygen, surface hydroxyl groups, and adsorbed methyl chloride. Such controlled experiments enable us to isolate various aspects of the photooxidation process and to definitively pinpoint the role of each species involved in the surface photochemical process. Our results suggest that the surface oxygen vacancies are the photocatalytic sites. Molecular oxygen adsorbed on these sites is the primary photochemical oxidizing agent. The surface hydroxyl groups derived from water are not photocatalytically reactive under the conditions of our investigation based on ^{18}O isotopic labeling in these groups. The photochemical process is induced by the band-gap excitation of the TiO_2 semiconductor.

Experimental Section

The experiments were performed in a stainless steel ultrahigh vacuum (UHV) chamber with a base pressure of less than 1×10^{-10} mbar. Details of the experimental setup and crystal preparation will be reported elsewhere.[24] Briefly, the system[25] is equipped with (1) a Perkin-Elmer digitally controlled cylindrical mirror analyzer (CMA) for Auger electron spectroscopy (AES), (2) a home-built low energy electron diffraction (LEED) apparatus for structural characterization, (3) a UTI 100C quadrupole mass spectrometer (housed in a differentially pumped shield with a 1.6-mm aperture[26]) multiplexed with a VTI computer interface for temperature programmed desorption (TPD) measurements, (4) an ion gun for Ar^+ sputter cleaning, and (5) a collimated and calibrated microcapillary array doser for accurate gas exposure to the crystal surface.[27-30]

The $TiO_2(110)$ single crystal was obtained from Commercial Crystal Laboratories, Inc. (the total impurity level is less than 50 ppm with Si as the largest impurity at ~20 ppm), and is

---

[⊗] Abstract published in *Advance ACS Abstracts,* May 1, 1995.

0022-3654/95/2099-7626$09.00/0

mounted onto a Ta support plate for heating and cooling. The crystal is mounted in such a way that no part of the support is exposed and only the front face of the crystal is seen in TPD measurements, Auger measurements, gas dosing (using the beam doser), or photon exposures. The temperature of the crystal is measured by a type-K thermocouple inserted into a precut slot at one corner of the crystal. The thermocouple is fixed with a high temperature ceramic adhesive (AREMCO 571) which has nearly the same thermal conductivity and thermal expansion coefficient as TiO_2. The crystal temperature can be linearly ramped between 100 and 1000 K. The heating rate in the TPD measurements reported here is 0.5 K/s. The crystal is cleaned by Ar^+ sputtering. The defect-free (oxidized) surface is obtained by annealing the clean surface in an O_2 flux to 900 K followed by continuous exposure to O_2 at 300 K for at least 1 h. The surface thus prepared shows a sharp (1 × 1) LEED pattern. The surface defects are produced by annealing the above surface to 900 K at a heating rate of 0.5 K/s. Ultraviolet photoemission spectroscopy,[31] X-ray photoemission spectroscopy (XPS),[32] ion scattering spectroscopy (ISS),[32] and chemisorption experiments[33] have shown that this annealing process produces surface oxygen vacancies.

The photochemistry is performed using a 350-W high pressure Hg arc UV lamp (Oriel Inc.). The lamp produces UV radiation above 230 nm (photon energies of less than 5.40 eV). The UV beam from the source passes through a water filter (4 cm) and an additional 100% infrared blocking filter. The UV beam is then focused onto the crystal in the UHV chamber through a sapphire window. The full arc is used in all the experiments except for the energy dependent study, where a set of interference filters (fwhm < 12 nm) are placed in the beam path in front of the sapphire window. The UV beam and the crystal can be configured for normal incidence to achieve maximum photoreaction or for irradiation when the crystal is line-of-sight with the apertured QMS so that the photodesorbing species can be monitored. The energy density of the UV beam is continuously measured with a Si photodiode detector and is calibrated with a photothermopile detector.[25] Energy densities of 0.24 $J/(s \cdot cm^2)$ are received by the crystal when the full-arc UV beam is used.

For photoexperiments, the crystal at 105 K has been exposed to the molecules as indicated on each spectrum (e.g., "D_2O + O_2 + CH_3Cl" means that the surface is first dosed with D_2O, and then O_2, and then CH_3Cl). This surface is then irradiated with the full-arc UV beam for 10 min. The temperature of the crystal never exceeds 130 K during the photoirradiation, and no thermal desorption effects occur during irradiation. A TPD spectrum of the parent CH_3Cl molecule and the product molecule is then recorded. For each photoexperiment, a reference TPD spectrum is taken with exactly the same procedure but without the 10 min of UV irradiation. The TPD spectrum with UV irradiation (labeled as "photo") is then compared to the reference TPD spectrum (labeled as "dark") to illustrate the consumption of the parent CH_3Cl molecules during photoirradiation. The results are presented as pairs of TPD spectra. Each pair corresponds to one specific combination of gas exposures (e.g., "CH_3Cl only" or "O_2 + CH_3Cl"). The methyl chloride coverage in all the experiments reported here is less than 0.25 monolayer.

Results

The key issues addressed here are as follows: (1) what are the photocatalytically active sites on the TiO_2 surface, (2) what are the reactive species in the photooxidation process, and (3) what is the excitation mechanism? Figures 1 and 2 compare the effects of the surface defects, the surface hydroxyl groups, and the adsorbed molecular oxygen on the photoreaction.

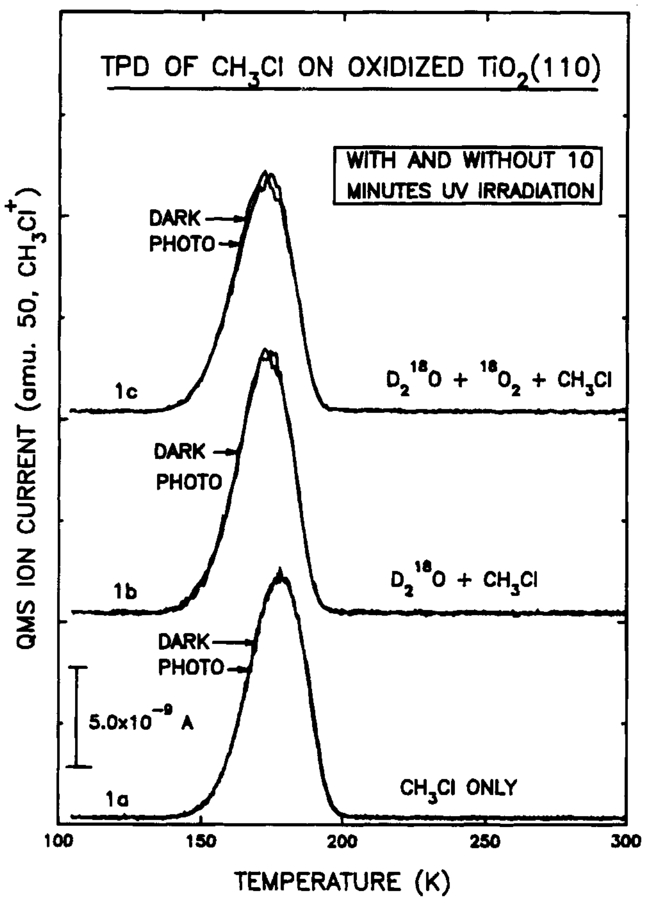

Figure 1. Comparison of methyl chloride TPD spectra following a 10-min UV irradiation (PHOTO) to that without UV irradiation (DARK) on an *oxidized* $TiO_2(110)$ surface. Gas exposures are as follows: 1a, 2.75×10^{13} CH_3Cl/cm^2; 1b, 5.84×10^{13} $D_2{}^{18}O/cm^2$ + 2.75×10^{13} CH_3Cl/cm^2; 1c, 5.84×10^{13} $D_2{}^{18}O/cm^2$ + 4.56×10^{13} $^{18}O_2/cm^2$ + 2.75×10^{13} CH_3Cl/cm^2.

In Figure 1, the TPD spectra of CH_3Cl from an oxidized (defect-free) $TiO_2(110)$ surface are presented. Spectra pair 1a is produced with CH_3Cl as the only adsorbed species. It is quite obvious that the PHOTO spectrum is essentially identical to the DARK spectrum. This result indicates that CH_3Cl does not photodissociate or photodesorb on the $TiO_2(110)$ surface within the photon energy range of our experiment. Nor is there any thermal desorption induced due to the temperature change during UV irradiation. Similarly, no change is observed between the photo and dark spectra in spectra pairs 1b and 1c for the coadsorption of $D_2{}^{18}O$ + CH_3Cl and $D_2{}^{18}O$ + $^{18}O_2$ + CH_3Cl, respectively, on the defect-free surface. The shift of the desorption peak to a slightly lower temperature is due to coadsorbed $D_2{}^{18}O$. We have shown in separate work that repulsive effects exist between adsorbed water and methyl chloride which shifts the methyl chloride desorption peak to successively lower temperatures with increasing water coverages.[24]

Figure 2 compares the photoinduced changes in the TPD spectra of methyl chloride on the annealed surface (containing oxygen vacancies or surface defects). The surface is annealed to 900 K at a temperature scan rate of 0.5 K/s to produce defect sites and then cooled over a time period of 450 s to 105 K before it is exposed to the gases indicated. The desorption temperature of methyl chloride on the defective surface is about 14 K higher than that in Figure 1, suggesting that methyl chloride binds more strongly to the defective surface than to

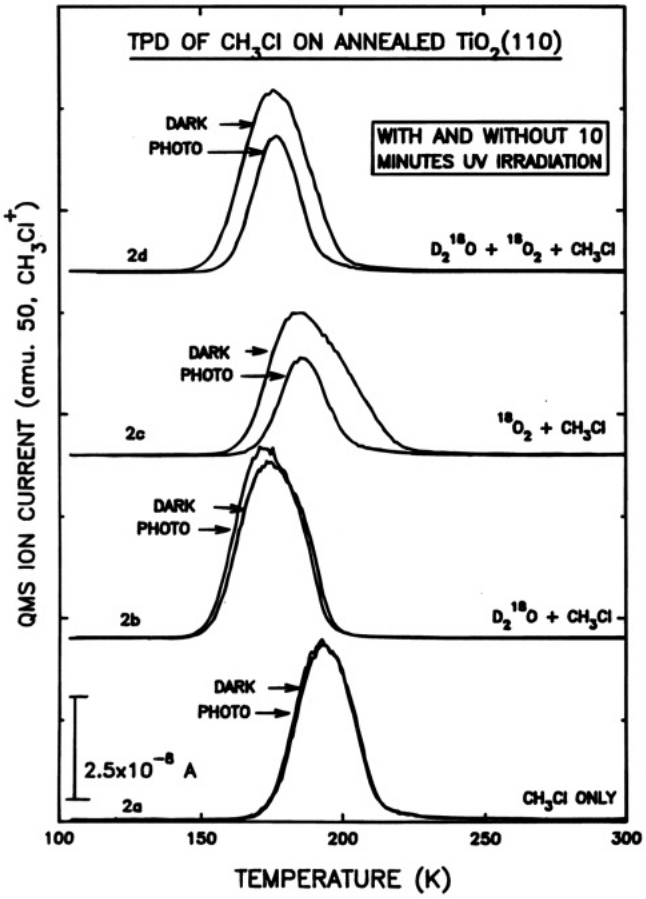

Figure 2. Comparison of methyl chloride TPD spectra following a 10-min UV irradiation (PHOTO) to that without UV irradiation (DARK) on an *annealed* $TiO_2(110)$ surface. Gas exposures are as follows: 2a, 3.85×10^{13} CH_3Cl/cm^2; 2b, 5.84×10^{13} $D_2{}^{18}O/cm^2 + 3.85 \times 10^{13}$ CH_3Cl/cm^2; 2c, 4.56×10^{13} ${}^{18}O_2/cm^2 + 3.85 \times 10^{13}$ CH_3Cl/cm^2; 2d, 5.84×10^{13} $D_2{}^{18}O/cm^2 + 4.56 \times 10^{13}$ ${}^{18}O_2/cm^2 + 3.85 \times 10^{13}$ CH_3Cl/cm^2.

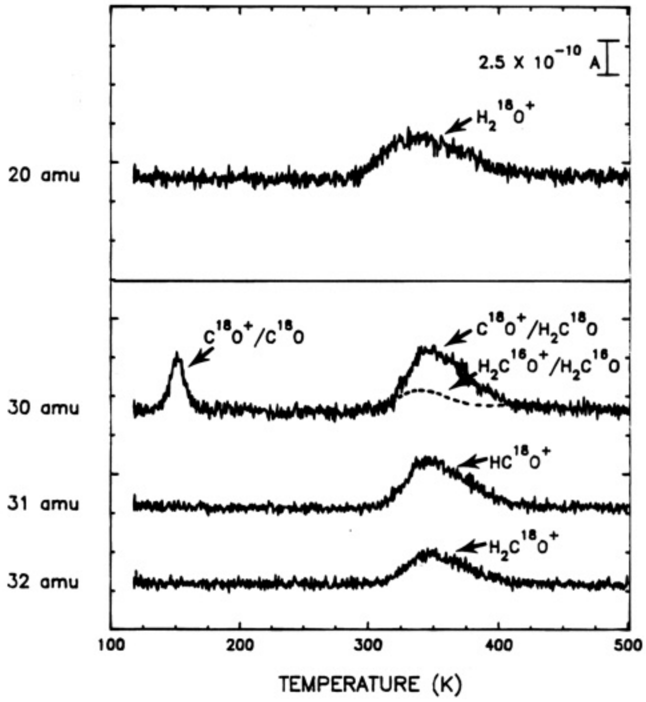

Figure 3. Thermal desorption yield of formaldehyde, CO, and water following 10-min UV irradiation of the annealed $TiO_2(110)$ surface preadsorbed with 4.56×10^{13} ${}^{18}O_2/cm^2 + 3.85 \times 10^{13}$ CH_3Cl/cm^2.

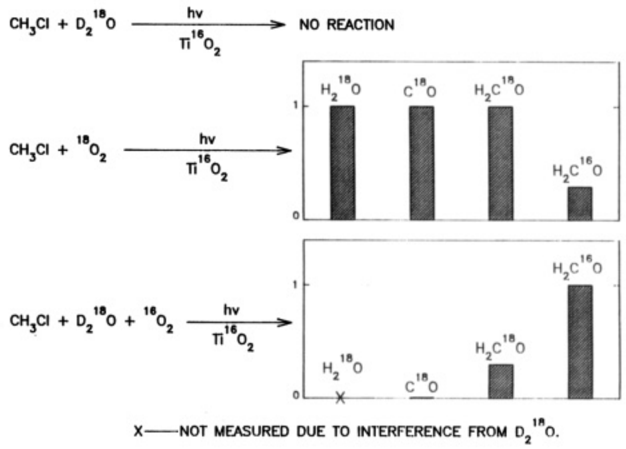

Figure 4. Schematic illustration of the isotope distribution in the photochemical products.

the oxidized surface. When only methyl chloride is adsorbed on the defective surface (spectra pair 2a), no change in the TPD spectrum is induced during photoirradiation. Spectra pair 2b is produced from the coadsorption of $D_2{}^{18}O + CH_3Cl$. Again, the change in the TPD spectrum, especially the total area of the CH_3Cl desorption peak, is negligible. The shift of the desorption peak to slightly lower temperature as compared to 2a is due to coadsorbed $D_2{}^{18}O$ (as mentioned previously).

For spectra 2c, a large decrease in the area of the CH_3Cl desorption peak is observed after photoirradiation of coadsorbed ${}^{18}O_2 + CH_3Cl$. Thus, methyl chloride is consumed during the photoirradiation in the presence of adsorbed oxygen. Spectra pair 2d shows a similar change for the coadsorption of $D_2{}^{18}O + {}^{18}O_2 + CH_3Cl$ after photoirradiation. Line-of-sight QMS measurements made during photoirradiation show no increase for *m/e* 50 (CH_3Cl^+) or 15 ($CH_3{}^+$) signals, indicating that no photodesorption or photofragmentation occurs. A sensitivity analysis of this measurement indicates that photodesorption processes with cross sections in the 10^{-20}-cm^2 range would have been detected. Even if a photodesorption or photofragmentation process with a cross section of 10^{-20} cm^2 did occur, the maximum contributions of such a process would be less than 8% of the observed *change* in the TPD peak area of CH_3Cl.

Experiments performed following photoirradiation of ${}^{18}O_2 + CH_3Cl$ show that formaldehyde ($H_2C^{18}O$), carbon monoxide ($C^{18}O$), and water are the major products and these products are detected by postirradiation TPD experiments, as shown in Figure 3. A $H_2{}^{18}O$ (amu 20) desorption peak centered at ~330 K is shown in the upper panel. Molecular $C^{18}O$ is also produced, as evident from the $C^{18}O^+$ (amu 30) desorption peak at ~140 K, which is typical of weakly adsorbed CO on the $TiO_2(110)$ surface. The formation of formaldehyde ($H_2C^{18}O$) is confirmed by the observations of $H_2C^{18}O^+$ (amu 32) and its cracking pattern $HC^{18}O^+$ (amu 31) and $C^{18}O^+$ (amu 30), all at ~340 K. For the amu 30 desorption peak at 340 K, approximately 30% of the intensity is due to a contribution from $H_2C^{16}O^+$, suggesting that lattice oxygen is also involved in a minor reaction channel for the formation of formaldehyde. This 30% intensity contribution for amu 30 corresponds to an isotope distribution of about 70% $CH_2{}^{18}O$ + 30% $CH_2{}^{16}O$. HCl (mass 36, 38) is also an expected product but is not detected during TPD measurement due to its low yield and high sticking probability onto the chamber walls. However, we do observe an increase in the background HCl level after a long period of photooxidation experiments.

Figure 4 schematically shows the isotope abundance of the photochemical products. No reaction is observed when coadsorbed $CH_3Cl + D_2{}^{18}O$ is UV-irradiated. When CH_3Cl is UV-

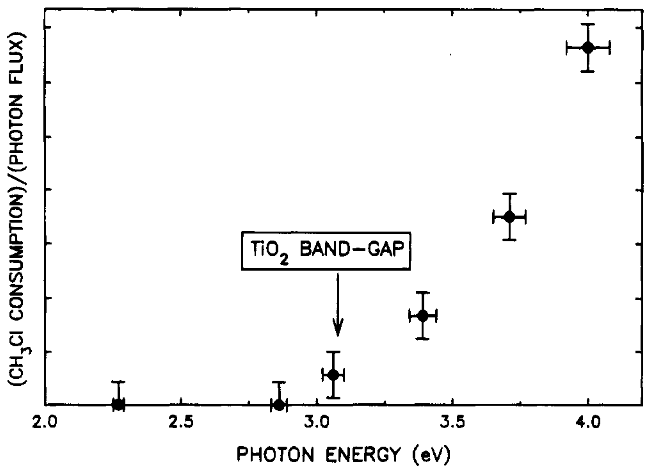

Figure 5. Energy dependence of the normalized photoreaction yield. The photoreaction extent is measured by normalizing the decrease in the CH_3Cl TPD peak area against the photon flux for a 10-min photoirradiation period. $D_2{}^{18}O + {}^{18}O_2 + CH_3Cl/TiO_2(110)$.

irradiated in the presence of adsorbed $^{18}O_2$, the products $H_2{}^{18}O$, $C^{18}O$, and formaldehyde (70% $H_2C^{18}O$ and 30% $H_2C^{16}O$) are observed. When CH_3Cl is photooxidized in the presence of $D_2O^{18} + {}^{16}O_2$, no $C^{18}O$ is formed and the ratio of $H_2C^{18}O$ and $H_2C^{16}O$ is reversed (30% $H_2C^{18}O$ and 70% $H_2C^{16}O$). This indicates that the oxygen in the CO products is exclusively from the molecular oxygen, while the oxygen in the formaldehyde products can be from adsorbed water, O_2, or the lattice. The result suggests that the formation of CO and formaldehyde occurs via different channels. CO may be produced from direct attack of CH_3Cl by the activated O_2 species. H_2CO may be formed from a currently unknown intermediate which is produced initially by the reaction with activated O_2 species and which further undergoes reaction with O_2, adsorbed water, or lattice oxygen in the thermal desorption process to produce H_2CO. Details of the reaction channel analysis will be presented in a later paper.[24]

In Figure 5, the extent of CH_3Cl photooxidation for the $D_2{}^{18}O + {}^{18}O_2 + CH_3Cl$ system is plotted against the incident photon energy. The reaction extent is measured as the decrease in the methyl chloride TPD peak area due to photooxidation normalized against the incident photon flux. The plot clearly demonstrates that no photooxidation occurs for photon energies of less than 3.0 eV. The reaction yield dramatically increases for photon energies higher than 3.1 eV. This threshold energy corresponds to the band-gap of the rutile TiO_2 solid, indicating that band-gap excitation of TiO_2 causes the photooxidation process. Direct photochemical excitation of neither CH_3Cl nor O_2 would occur at photon energies near 3.1 eV. The photoreaction yield increases above the threshold energy of 3.1 eV. A similar wavelength dependence involving a gradual increase in photoyield above the threshold has been observed in several studies, including the photoproduction of H_2 on Pt/TiO_2,[34] photocurrent measurements on a single crystal TiO_2 electrode,[35] and the photodesorption yield of CO_2 [36] and O_2 [37] on TiO_2 powders. The dependence is probably due to an increasing overlap of the photoelectron produced in the solid with a broadened acceptor level in chemisorbed O_2 as the photoelectron energy is increased above the threshold.

Discussion

1. Catalytic Sites for Photooxidation. We have demonstrated that photooxidation of CH_3Cl on $TiO_2(110)$ occurs only on the annealed surface in the presence of adsorbed oxygen. This shows that the photocatalytic sites exist only on the annealed surface. The annealing process produces surface oxygen vacancies.[31-33] These oxygen vacancies are Ti^{3+} point defects which are generated by eliminating surface oxygen atoms by thermal desorption. Ultraviolet photoemission spectroscopy (UPS) studies have observed the growth of a surface state at 0.8 eV below the Fermi level after the surface is annealed to high temperatures.[31] This state can be eliminated by adsorption of oxygen or water.[31] Using $^{18}O_2$ and $H_2{}^{18}O$ adsorption, the incorporation of ^{18}O atoms into the surface lattice was observed in ISS studies.[32] It is also observed that the chemisorption of oxygen-containing molecules on the annealed surface preferentially undergoes O atom extraction from adsorbed H_2O, CH_2O, and NO to produce H_2, C_2H_4, and N_2O, respectively.[33] However, no such chemical interactions are observed on the oxidized surface. The above results suggest that the annealed surface is oxygen deficient, consistent with the oxygen vacancy model of the annealed surface. Our observation of a photochemical process only on the annealed surface indicates that the oxygen vacancies are the photocatalytic sites.

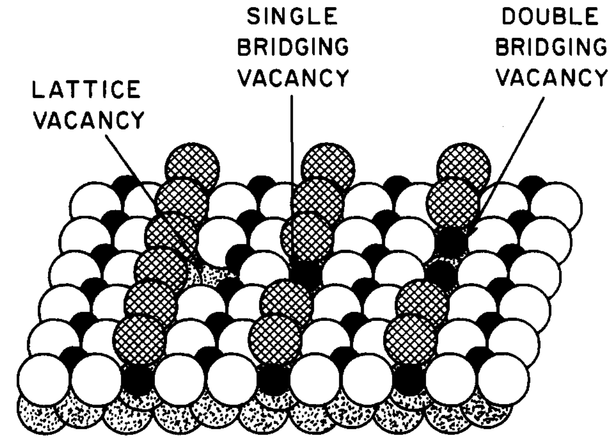

Figure 6. Structural model of the $TiO_2(110)$ surface. Three types of defects are shown: single bridging oxygen vacancy site, double bridging oxygen vacancy site, and single lattice oxygen vacancy site.

Figure 6 shows a structural model of the $TiO_2(110)$ surface. The oxidized (defect-free) surface is composed of rows of bridging oxygen atoms on top of the surface layer. Two types of defect sites can be produced by the removal of either a bridging oxygen atom or an in-plane lattice oxygen atom.[38] The removal of a bridging oxygen atom reduces the coordination number of two 6-fold Ti cations to 5. The removal of an in-plane lattice oxygen atom reduces the coordination number of two 5-fold Ti cations to 4 and one 6-fold Ti cation to 5. The latter case is less favorable due to the formation of more coordinatively unsaturated Ti cations. Furthermore, it is energetically more costly to remove an in-plane lattice oxygen since it is coordinated to three Ti cations while a bridging oxygen is only coordinated to two Ti cations. Although both types of oxygen vacancies can be produced, the relatively low temperature for producing the active defect sites (starting temperature ~500 K [33]) indicates that a bridging oxygen vacancy is more probable for mild thermal activation. However, a distinction between the two types of defect sites will require further study using other measurement methods.

2. Role of Surface Hydroxyl Groups and Adsorbed O_2. In most of the photooxidation studies, surface hydroxyl groups and gas-phase oxygen are present in the reaction system. Consequently, the role of these two species become a key issue in elucidating the mechanism of the catalytic photooxidation process and, therefore, has been the focus of many kinetics investigations.

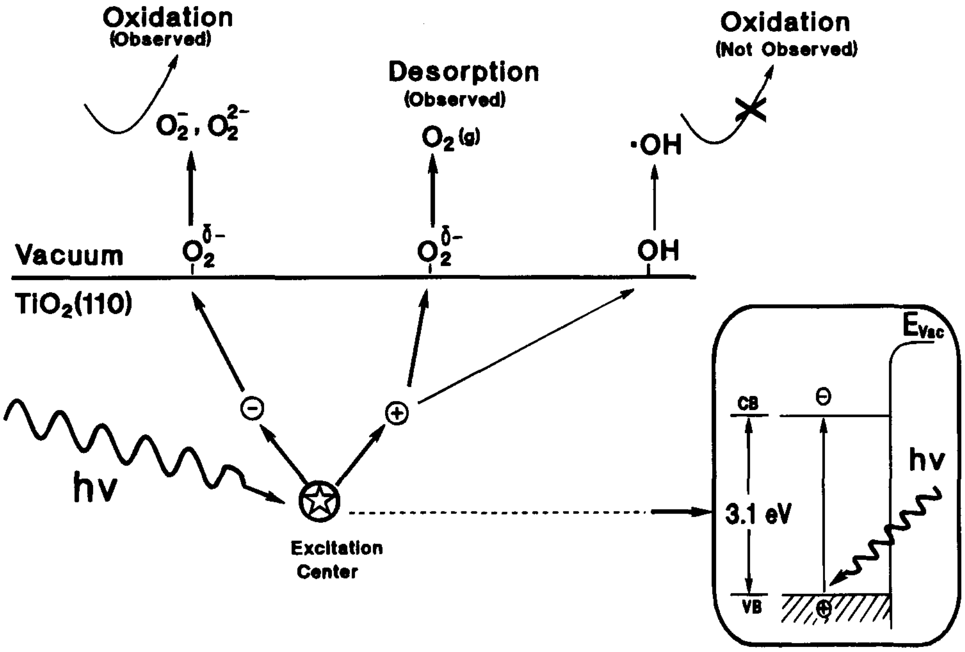

Figure 7. Schematic illustration of the photooxidation process induced by the TiO_2 band-gap excitation.

Using isotopically labeled oxygen, we are able to distinguish the origin of the oxygen atoms in the photooxidation intermediates and products. Our experimental data reveal two important aspects of this issue: (1) The photooxidation of CH_3Cl can be achieved in the absence of surface hydroxyl groups and water but not in the absence of O_2. This indicates that the photoactivated surface oxygen species are essential, while surface hydroxyl groups are not as important for the photooxidation process. (2) When both hydroxyl groups (or water) and adsorbed O_2 are present on the surface, oxygen in O_2 is more extensively incorporated into the photooxidation products. More explicitly, the oxygen atoms in the oxidation product CO originate exclusively from O_2, while the oxygen in the oxidation product CH_2O is mostly from O_2 and partially from water and lattice oxygen. This clearly demonstrates that the adsorbed molecular oxygen plays a more important role than the surface hydroxyl groups.

These experimental observations enable us to test whether the existing model for TiO_2-based photooxidation can be applied here. In this model,[5,6] the photogenerated electrons are trapped at surface oxygen vacancy sites and then removed by oxygen through an interfacial electron transfer process. Molecular oxygen is therefore believed to be an electron scavenger in the system,[39,40] promoting hole lifetime and increasing the photoefficiency. In this model, the photogenerated holes in the TiO_2 valence band then react with surface hydroxyl groups to produce •OH radicals. These hydroxyl radical species are highly reactive and can oxidize organic species on the surface or in the solution. In this mechanism, the oxygen atom in the surface hydroxyl groups or adsorbed water will appear in the oxidation products and the oxygen atoms in the adsorbed molecular oxygen are less likely to be included in the products.

This prediction is obviously inconsistent with our experimental observations. We have shown that surface hydroxyl groups are not necessary to achieve photooxidation of CH_3Cl, and the oxygen in O_2 is more extensively included in the oxidation products. The above reaction scheme may therefore not be applied for the photooxidation of CH_3Cl on $TiO_2(110)$. This conclusion, together with the findings in previous investigations,[22,23] suggests that the photooxidation process at the gas–solid interface may follow a different reaction mechanism.

3. Band-Gap Excitation Induced Surface Chemistry. Methyl chloride can be photooxidized on the TiO_2 surface. This process has an energy threshold of ~3.1 eV (Figure 5), consistent with band-gap excitation of bulk TiO_2. The direct photofragmentation of methyl chloride is not possible within the photon energy range (<5.40 eV) of this study.[41] Electron attachment induced dissociation of methyl chloride[42] does not occur on the $TiO_2(110)$ surface in our studies since no photoreaction is observed when only methyl chloride is adsorbed on the surface.

The importance of molecular oxygen in the oxidation process is demonstrated by the overall photoreactivity of oxygen on the TiO_2 surface and its involvement in the final products. Experiments without UV irradiation show that no thermal reaction occurs between adsorbed methyl chloride and adsorbed oxygen. The production of excited state O_2 and/or negative ions of O_2 is the key step in the oxidation process. While direct excitation of molecular oxygen is possible within the photon energy range of our study,[43] a threshold of 3.1 eV for the photochemical reaction is inconsistent with the direct excitation of the chemisorbed molecular O_2. Thus, substrate TiO_2 mediated excitation is the dominant process.

Molecular oxygen adsorbs at the defect Ti^{3+} sites, as shown schematically in Figure 7. Partial electron transfer to produce a $O_2^{\delta-}-Ti^{(3+\delta)+}$ complex is the driving force for stabilizing O_2 on the surface.[44,45] Under UV irradiation, adsorbed O_2 can either capture electrons to produce O_2^- and/or O_2^{2-} or capture a hole[36,37] to produce neutral O_2. The formation of these ionic radicals has been confirmed in several previous studies.[15,20,21,46–50] The anionic O_2 species are chemically reactive and are strong oxidizing agents. We have observed desorption of neutral molecular oxygen during the photooxidation process.[24] This photodesorption process also has a threshold energy of 3.1 eV. The exclusive involvement of molecular oxygen in both the surface oxidation and photodesorption process indicates that adsorbed O_2 may indeed act as both an electron and hole acceptor. As an electron acceptor, O_2^- or O_2^{2-} species are produced which further oxidize adsorbed organic species. Further photodissociation of the protonated oxygen anions (HO_2, H_2O_2) may be the source of •OH radicals detected in aqueous suspensions.[20] As a hole acceptor, neutral O_2 is produced which then mainly undergoes photodesorption.[37] Other channels of hole trapping have also been reported in the literature. One of these involved the formation of a O_3^- species by $h^+ + O^{2-}(\text{lattice}) + O_2 \rightarrow O_3^-$.[21,47,48] It has been shown that this radical species can oxidize CO to CO_2 and that only the oxygen originally from the gas-phase O_2 will be present in CO_2.[48]

Our findings are schematically summarized in Figure 7. This scheme for the photooxidation of methyl chloride on TiO_2 surfaces emphasizes the significant role of the adsorbed O_2. Although TiO_2 photocatalysts operating in solutions present a more complex system than that studied here, the fundamental principles and elemental steps shown in Figure 7 are likely to be involved in aqueous environments. The extension of these results to other chlorinated molecules awaits further work.

Conclusions

We have studied the roles of surface defects (surface oxygen vacancies), adsorbed molecular oxygen, and surface hydroxyl groups in the photooxidation of methyl chloride on the TiO_2(110) surface. The following results have been found:

1. Surface oxygen vacancies and molecular oxygen adsorbed at these defect sites are found to be an essential combination for the photooxidation reaction to initiate and to proceed.

2. The surface hydroxyl groups play a far less significant role and do not photooxidize methyl chloride. However, adsorbed water molecules do participate in the photooxidation channel, leading to formaldehyde product in the presence of adsorbed molecular oxygen.

3. The photooxidation products observed from CH_3Cl on $TiO_2(110)$ are CO, H_2CO, and H_2O.

4. The photooxidation has an energy threshold of 3.1 eV, indicating that the photochemical reaction is induced by TiO_2 band-gap excitation.

5. Substrate sensitized oxidation by chemisorbed molecular oxygen, as illustrated in Figure 7, is a key step in the photooxidation of methyl chloride on $TiO_2(110)$.

Acknowledgment. We would like to thank Professor M. A. Fox for her invaluable comments on this manuscript prior to submission for publication. We acknowledge with thanks the support of the Army Research Office.

References and Notes

(1) Fox, M. A.; Dulay, M. T. *Chem. Rev.* **1993**, *93*, 341.
(2) Serpone, N., Pelizzetti, E., Eds. *Photocatalysis-Fundamentals and Applications*; Wiley-Interscience: New York, 1989.
(3) Ollis, D. F.; Pelizzetti, E.; Serpone, N. *Environ. Sci. Technol.* **1991**, *25*, 1522.
(4) Legrini, O.; Oliveros, E.; Braun, A. M. *Chem. Rev.* **1993**, *93*, 671.
(5) Turchi, C. S.; Ollis, D. F. *J. Catal.* **1990**, *122*, 178.
(6) Pelizzetti, E.; Minero, C. *Electrochim. Acta* **1993**, *38* (1), 47.
(7) Angugliaro, V.; Palmisano, L.; Sclafani, A.; Minero, C.; Pelizzetti, E. *Toxicol. Environ. Chem.* **1988**, *16*, 89.
(8) Al-Ekabi, H.; Serpone, N.; Pelizzetti, E.; Minero, C.; Fox, M. A.; Draper, R. B. *Langmuir* **1989**, *5*, 250.
(9) Ollis, D. F.; Hsiao, C.; Budiman, L.; Lee, C. *J. Catal.* **1984**, *88*, 89.
(10) Barbeni, M.; Morello, M.; Pramauro, E.; Pelizzetti, E.; Vincente, M.; Borgarello, E.; Serpone, N. *Chemosphere* **1987**, *16*, 1165.
(11) Turchi, C. S.; Ollis, D. F. *J. Catal.* **1989**, *119*, 480.
(12) Minero, C.; Aliberti, C.; Pelizzetti, E.; Terzian, R.; Serpone, N. *Langmuir* **1991**, *7*, 928.
(13) Mills, A.; Morris, S.; Davies, R. *J. Photochem. Photobiol. A: Chem.* **1993**, *70*, 183.
(14) Ceresa, E. M.; Burlamacchi, L.; Visca, M. J. *J. Mater. Sci.* **1983**, *18*, 289.
(15) Jaeger, C. D.; Bard, A. *J. Phys. Chem.* **1979**, *83*, 3146. Anpo, M.; Shima, T.; Kubokawa, Y. *Chem. Lett.* **1985**, 1799.
(16) Micic, O. I.; Zhang, Y.; Cromack, K. R.; Trifunac, A. D.; Thurnauer, M. C. *J. Phys. Chem.* **1993**, *97*, 7277, 13284.
(17) Sclafani, A.; Palmisano, L.; Schiavello, M. *J. Phys. Chem.* **1990**, *94*, 829.
(18) Cunningham, J.; Srijaranai, S. *J. Photochem. Photobiol. A: Chem.* **1988**, *43*, 329.
(19) Draper, R. B.; Fox, M. A. *Langmuir* **1990**, *6*, 1396.
(20) Okamoto, K.; Yamamoto, Y.; Tanaka, H.; Tanaka, M.; Itaya, A. *Bull. Chem. Soc. Jpn.* **1985**, *58*, 2015. Okamoto, K.; Yamamoto, Y.; Tanaka, H.; Itaya, A. *Bull. Chem. Soc. Jpn.* **1985**, *58*, 2023.
(21) Anpo, M.; Chiba, K.; Tomonari, M.; Coluccia, S.; Che, M.; Fox, M. A. *Bull. Chem. Soc. Jpn.* **1991**, *64*, 543.
(22) Stafford, U.; Gray, K. A.; Kamat, P. V.; Varma, A. *Chem. Phys. Lett.* **1993**, *205*, 55.
(23) Dibble, L. A.; Raupp, G. B. *Environ. Sci. Technol.* **1992**, *26*, 492. Dibble, L. A.; Raupp, G. B. *Catal. Lett.* **1990**, *4*, 345. Phillips, L. A.; Raupp, G. B. *J. Mol. Catal.* **1992**, *77*, 297.
(24) Linsebigler, A.; Lu, G.; Yates, J. T., Jr. To be published.
(25) Hanley, L.; Guo, X.; Yates, J. T., Jr. *J. Chem. Phys.* **1989**, *91* (11), 7220.
(26) Lu, G.; Linsebigler, A.; Yates, J. T., Jr. *J. Vac. Sci. Technol. A* **1994**, *12* (2), 384.
(27) Bozack, M. J.; Muehlhoff, L.; Russell, J. N., Jr.; Choyke, W. J.; Yates, J. T., Jr. *J. Vac. Sci. Technol. A* **1987**, *5*, 1.
(28) Winkler, A.; Yates, J. T., Jr. *J. Vac. Sci. Technol. A* **1988**, *6*, 2929.
(29) Campbell, C. T.; Valone, S. M. *J. Vac. Sci. Technol. A* **1985**, *3*, 408.
(30) Smentkowski, V. S.; Yates, J. T., Jr. *J. Vac. Sci. Technol. A* **1989**, *7*, 3325.
(31) Kurtz, R. L.; Stockbauer, R.; Madey, T. E.; Roman, E.; de Segovia, J. L. *Surf. Sci.* **1989**, *218*, 178.
(32) Pan, J. M.; Maschhoff, B. L.; Diebold, U.; Madey, T. E. *J. Vac. Sci. Technol. A* **1992**, *10*, 2470.
(33) Lu, G.; Linsebigler, A.; Yates, J. T., Jr. *J. Phys. Chem.* **1994**, *98*, 11733.
(34) Sakata, T.; Kawai, T. In *Energy Resources Through Photochemistry and Catalysis*; Grätzel, M., Ed.; Academic Press: New York, 1983.
(35) Yoneyama, H.; Tamura, H. *Electrochim. Acta* **1975**, *20*, 341.
(36) Shapira, Y.; Cox, S. M.; Lichtman, D. *Surf. Sci.* **1976**, *54*, 43. Van Hieu, N.; Lichtman, D. *Surf. Sci.* **1981**, *103*, 535.
(37) Yanagisawa, Y.; Ota, Y. *Surf. Sci. Lett.* **1991**, *254*, L433.
(38) Henrich, V. E. *Rep. Prog. Phys.* **1985**, *48*, 1481.
(39) Gerischer, H.; Heller, A. *J. Phys. Chem.* **1991**, *95*, 5261.
(40) Gerischer, H. *Electrochim. Acta* **1993**, *38* (1), 3.
(41) Okabe, H. *Photochemistry of Small Molecules*; Wiley-Interscience: New York, 1978.
(42) Zhou, X. L.; Zhu, X. Y.; White, J. M. *Surf. Sci. Rep.* **1991**, *13*, 121.
(43) Herzberg, G. *Molecular Spectra and Molecular Structure: I, Spectra of Diatomic Molecules*, 2nd ed.; VNR: New York, 1950; p 446.
(44) Göpel, W.; Rocker, G. *J. Vac. Sci. Technol.* **1982**, *21*, 389.
(45) Göpel, W.; Rocker, G.; Feierabend, R. *Phys. Rev. B* **1983**, *28*, 3427.
(46) Bickley, R. I.; Stone, F. S. *J. Catal.* **1973**, *31*, 389. Bickley, R. I.; Munuery, G.; Stone, F. S. *J. Catal.* **1973**, *31*, 389.
(47) Courbon, H.; Formenti, M.; Pichat, P. *J. Phys. Chem.* **1977**, *81*, 550.
(48) Anpo, M.; Kubokawa, T.; Fujii, T.; Suzuki, S. *J. Phys. Chem.* **1984**, *88*, 2572.
(49) Howe, R. F.; Grätzel, M. *J. Phys. Chem.* **1987**, *91*, 3906.
(50) Nosaka, Y.; Fox, M. A. *J. Phys. Chem.* **1988**, *92*, 1893.

JP941686I